



Characteristic morphological patterns within adolescent idiopathic scoliosis may be explained by mechanical loading

Benedikt Schlager¹ · Florian Krump¹ · Julius Boettinger¹ · Frank Niemeyer¹ · Michael Ruf² · Sebastian Kleiner³ · Meinrad Beer³ · Hans-Joachim Wilke¹

Received: 8 August 2017 / Revised: 2 March 2018 / Accepted: 2 May 2018 / Published online: 5 May 2018
© Springer-Verlag GmbH Germany, part of Springer Nature 2018

Abstract

Purpose Adolescent idiopathic scoliosis (AIS) is a three-dimensional deformity of the spine which exhibits morphological changes during growth. The goal of this study was to identify morphological patterns that could be explained by different loading patterns for AIS.

Methods Computed tomography data of 21 patients with diagnosed AIS and 48 patients without any visual spinal abnormalities were collected prospectively. The bony structures were reconstructed, and landmarks were placed on characteristic morphological points on the spine. Multiple morphological parameters were calculated based on the distances between the landmarks. The intra- and inter-observer variability for each parameter was estimated. Differences between healthy and scoliotic spines were statistically analysed using the *t* test for unpaired data, with a significance level of $\alpha = 0.01$.

Results Within the healthy group, an out-of-plane rotation of the vertebrae in the transverse plane was measured ($2.6^\circ \pm 4.1^\circ$ at T2). Relating the length of the spinal curvature to the T1–S1 height of the spine revealed that scoliotic spines were significantly longer. However, the endplate area in the AIS group was significantly smaller once compared to the curvature length. The relation between the left and right pedicle areas varied between 2.5 ± 0.79 and 0.4 ± 0.19 , while the ratio of the facet articular surfaces varied within 2.3 ± 0.5 and 0.5 ± 0.2 .

Conclusions This study identified a certain morphological pattern along the spine, which reveals a distinct load path prevalent within AIS. The data suggested that the spine adapts to the asymmetric load conditions and the spine is not deformed by asymmetric growth disturbance.

Graphical abstract These slides can be retrieved under Electronic Supplementary Material.

The graphical abstract consists of three slides from a presentation. The first slide, titled 'Key points', lists three main findings: 1. AIS is a 3D deformity with growth-related changes; 2. The study aimed to identify loading patterns for AIS; 3. Morphology parameters were obtained from CT scans of 21 AIS patients and 48 healthy patients. The second slide, titled 'Morphology parameters', shows diagrams of spine curvatures with various landmarks and parameters labeled. It includes a legend for 'Healthy' (black) and 'Scoliotic' (green) spine types and a caption explaining that parameters are grouped by main scoliotic curvature position (top, middle, bottom) and AIS location (thoracic, lumbar, thoracolumbar). The third slide, titled 'Take Home Messages', lists four key takeaways: 1. Morphological patterns reveal a distinct load path in AIS; 2. Spines initially classified as non-scoliotic show deformation and rotation similar to scoliotic spines; 3. Scoliotic spines adapt to asymmetric load conditions; 4. The study's morphology data provides a basis for developing scoliotic spine models.

Keywords Biomechanics · Spine · Morphology · Anatomy · Adolescent idiopathic scoliosis

Electronic supplementary material The online version of this article (<https://doi.org/10.1007/s00586-018-5622-0>) contains supplementary material, which is available to authorized users.

Extended author information available on the last page of the article

Introduction

Adolescent idiopathic scoliosis (AIS) is a three-dimensional deformity of the spine, which could exhibit distinct morphological characteristics compared to the symmetric

spine during growth. In 85% of the cases, the cause of adolescent scoliosis is unknown (idiopathic). According to Wolff's law, the morphological changes of bone should be influenced by the mechanical stimuli to which the bone is locally exposed to [1–3]. The morphology, therefore, might tell a story how intrinsic forces deform the spine and thereby gradually cause the formation of scoliotic deformities. Understanding the morphological characteristics of scoliotic spines might help to identify the pathology of AIS. Furthermore, knowledge concerning the shape of the bone is necessary for the development of in vitro [4] and numerical models of scoliotic spines [5], as well as for the classification of scoliotic curvatures [6].

The existing literature relating to the morphological characteristics of scoliotic spines focuses on the wedging and rotation of the vertebral bodies and discs, as well as the pedicle size. The spinal segment at the apex of a curve exhibits the strongest wedging, in which the vertebral body height on the concave side is smaller compared to the opposite side [7, 8]. Within the thoracic region, the wedging of the vertebral body is most profound, whereas in the lumbar region the disc is more wedged [9]. This deformation of the vertebrae and discs generally increases with the Cobb angle [10] and depends on the axial load it is exposed to [11].

In conjunction with a lateral displacement of the spine in the coronal plane, the vertebrae often rotate out of the sagittal plane towards the convexity of a curve [12].

A further characteristic of scoliotic vertebrae is the asymmetrical orientation and the size of the pedicles around the apex. The pedicle size on the concave side is smaller compared to the convex side [13–15]. Parent et al. [16] also investigated differences in the size of the facet joints, though no correlation could be found between the convexity and concavity. Even abnormalities in the cancellous bone structure of scoliotic spines were reported [17, 18].

Further studies measured the length differences between the anterior and posterior spinal columns [19–22]. Their findings lead to the hypothesis of an “anterior over-growth”, which refers to a longer anterior spinal column compared to the posterior column and spinal canal.

While the literature data indicate that scoliotic spines exhibit common morphological characteristics, it is not yet fully understood how these overall patterns are associated with the scoliotic shape and type.

The goal of this study was to quantify and identify morphological patterns within AIS patients in comparison with healthy spines, which might reveal a certain loading condition along the spine. Furthermore, these data provide an important basis for the generation of realistic scoliotic spine models.

Methods

Morphology parameters of the spine were obtained by evaluating computed tomography (CT) images of 21 patients diagnosed with AIS (“AIS” group) and 48 patients without any visible spinal abnormalities (“healthy” group) (ethical votes: 418/15-Zo/Sta and B-F-2016-053). The CT data were collected from the radiology departments retrospectively, whereby no CT scan was performed specifically for this study. Inclusion criteria for the CT data were a slice thickness of ≤ 1 mm and visibility of the spinal levels T1 to S1, including the whole chest. The mean age was 15 ± 2 years for the AIS group and 23 ± 12 years for the healthy group. To reduce variability in the data, the AIS cases were subdivided into the three groups lumbar ($n=5$), thoracic ($n=12$) and thoracolumbar ($n=4$), depending on the location of the main curvature.

Morphology analysis

The skeletal structure was reconstructed from the CT data using the software tool AVIZO (release: 8.0; FEI Visualization Sciences Group, Hillsboro, Oregon, USA). Landmarks were placed manually on predefined characteristic morphological points on the spine and chest (Fig. 1). Morphological parameters were then derived from the coordinates of those landmarks.

In this study, we focused the analysis on the overall dimensions of the spine, the shape of the vertebrae and discs, as well as the cross-sectional area of pedicles and the articular facet joint surface area. An average endplate size for each spine was calculated as by summarizing the endplate area at each vertebral level i for all levels m (sup: superior, inf: inferior).

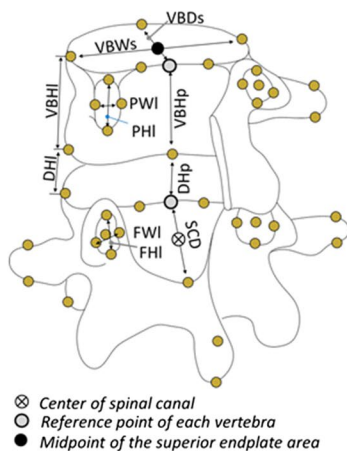
$$\bar{A} = \frac{1}{m} \sum_{i=1}^m \frac{A_{i,\text{sup}} + A_{i,\text{inf}}}{2}$$

The endplate area was assumed to have an elliptical shape.

To investigate potential length differences between the anterior and posterior spinal columns, the length of the spinal canal was quantified by connecting the centre of the spinal canal at each vertebral level. The centre of the spinal canal was positioned in midline: between the posterior tip of the canal on the lamina and the point on the posterior edge of the superior endplate (see Fig. 1).

In addition, the individual length of the spinal curvature and height of the spine was calculated (Fig. 2a). To reduce parameter variations between the patients, a

Fig. 1 Left: position of the landmarks on a vertebral segment and morphologic parameters which were calculated from these landmarks. Right: table of parameters including their averaged inter and intra-observer variability of 12 ($n=2 \times 6$) measurements



Parameter	Abbr.	Rater Variability [%]
Vertebral body height posterior	VBHp	2.4
Vertebral body height left	VBHI	2.6
Vertebral body width superior	VBWs	1.8
Vertebral body depth superior	VBDS	0.8
Disc height posterior	DHp	2.3
Disc height left	DHI	2.5
Facet height left	FHI	5.7
Facet width left	FWI	5.5
Pedicle height left	PHI	1.7
Pedicle width left	PWI	5.2
Spinal canal depth	SCD	1.7

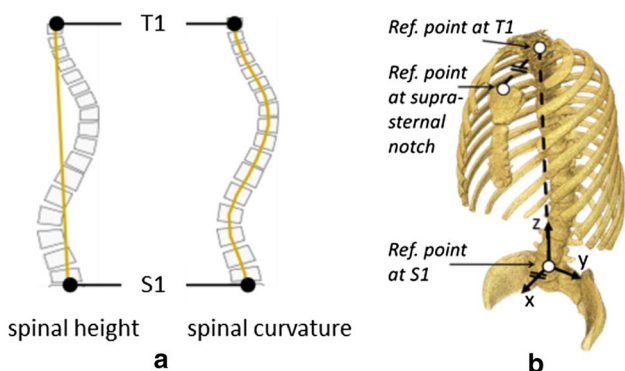


Fig. 2 **a** Sketch of the specified “spinal height” and “spinal curvature”. Each length was calculated in three-dimensional space: “spinal height” between mid of the superior endplates of T1 and S1, and the “spinal curvature” by connecting the mid-point of the superior endplate of each vertebra. **b** Orientation of the global coordinate system of each patient. The z-axis points from the middle of the posterior edge of the superior endplate of S1 to T1, while the sagittal plane was defined by the vector between T1 and the centre of the suprasternal notch. *Ref.:* Reference

patient-specific coordinate system was created using three landmarks (Fig. 2b).

Spinal parameters, such as the displacement in the coronal plane and rotation of the vertebrae, were measured relative to the superior endplate of S1.

Statistical analysis

The intra- and inter-observer variability for the placement of the landmarks was analysed by two observers who repeated the placement of the landmarks six times on a healthy and a scoliotic spine. This allowed the determination of measurement accuracy for each parameter.

The results of the healthy group were statistically analysed using a two-sided one-sample *t* test, by comparing the values to an expected true mean.

To identify significant differences between the healthy and scoliotic spines, the mean values at each level were compared using the *t* test for unpaired data. A significance level of 0.01 was considered. The statistical analysis was performed using the SciPy package (version 0.16.0) [23] with Python (version 3.4.3).

Results

The absolute inter- and intra-observer variability of the parameters decreased with an increase in the distance between landmarks. Therefore, the highest deviation was observed for small parameters such as the disc height, with a variability of 3%, and the facet parameters, with a variability of about 6% of their total value (Fig. 1).

Healthy spine data

The lateral displacement, relative to the mid-sagittal plane of each individual coordinate system of the healthy patients, varied in the range of -1.3 ± 5.0 mm at T7 and 0.8 ± 3.4 mm at L4 (Fig. 3). Interestingly, the vertebrae of the healthy group exhibited an inherent rotation of the vertebrae which deviated significantly from zero at level T2 ($2.6^\circ \pm 4.3^\circ$, $p = 0.009$). It should be noted that the reduction in the lateral displacement to 0 at T1 is due to the reference coordinate system in which S1 and T1 are used as reference points.

The pedicle area ratio between the left and right sides was within the expected mean value of 1.0: between 0.9 ± 0.1 at T6 and 1.1 ± 0.2 at T1. The facet area ratio between the left and right sides varied between 0.9 ± 0.2 at T5 and 1.1 ± 0.3 at T12.

General length of the spine

Within the healthy group, the height of the spine from T1 to S1 correlated with the length along the spinal curvature

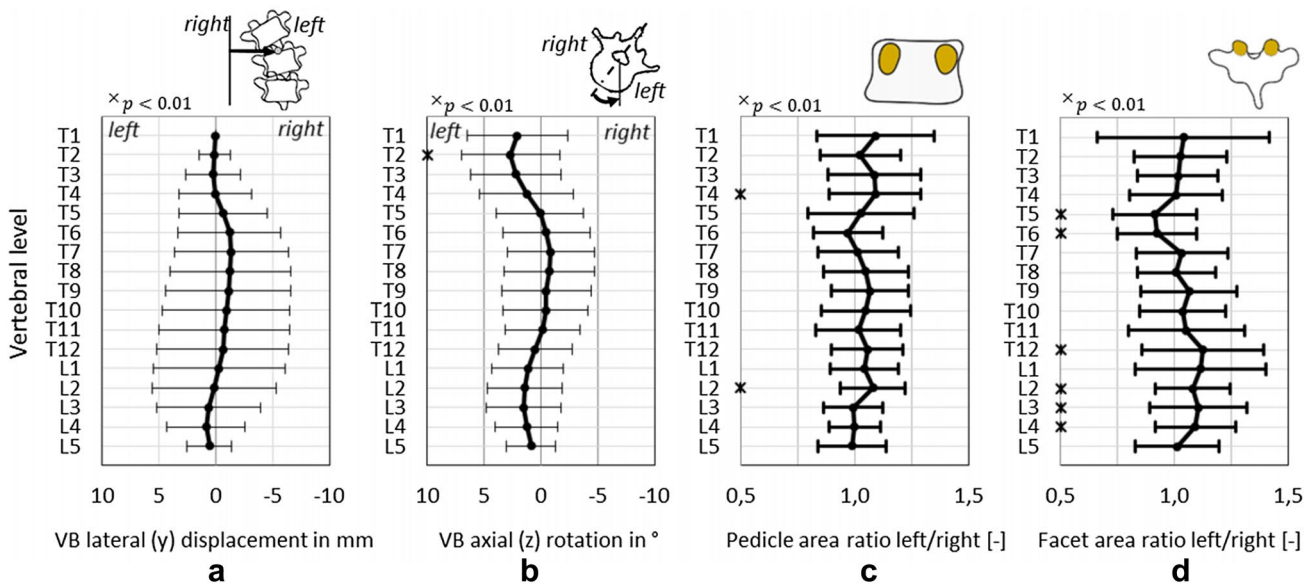


Fig. 3 Mean variation at each spinal level of the lateral displacement (a) and axial rotation (b) of the vertebral body (VB), as well as the ratio between left and right pedicles (c) and facet (d) areas for the healthy spine group

($r^2 = 0.99$). All scoliotic spines deviated from the almost perfectly linear relation present in the healthy group towards a disproportionately longer spinal curvature compared to their T1–S1 height (Fig. 4a).

A similar trend could be identified by comparing the length along the anterior edge of the spine with the length of the spinal canal, whereby a linear relation was present in the healthy group ($r^2 = 0.96$) (Fig. 4b). The average relation between the length along the anterior column and the spinal canal length was 1.10 ± 0.02 for healthy spines and 1.18 ± 0.08 for scoliotic spines. Within the thoracic and

thoracolumbar AIS group, it was found that this relation correlated significantly with the Cobb angle ($p < 0.01$, Pearson’s $r = 0.88$) (Fig. 4c).

Endplate

The averaged endplate area (\bar{A}) was compared to the height of the spine and the length of the spinal curvature (Fig. 5). No differences of the averaged endplate area in relation to the spinal height could be identified between the healthy and AIS groups. Yet, the endplate area was significantly smaller

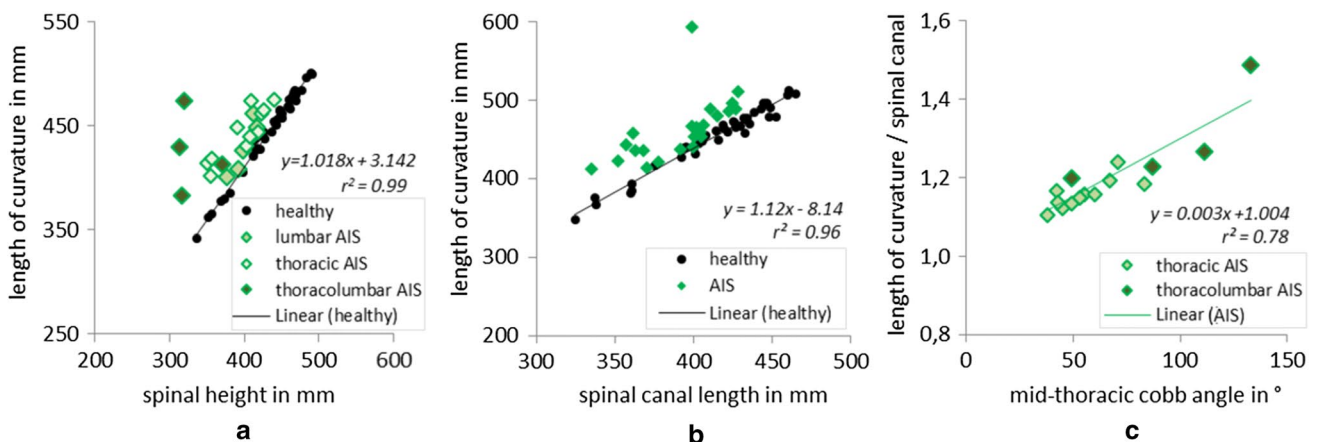


Fig. 4 a Relation between the length of the curvature and the spinal height for each spine. Linear regression was performed using the data of the healthy group. **b** Relation between the length along the anterior column and the spinal canal length. **c**. Relation between the length

of the anterior column and the length of the spinal canal compared with the Cobb angle in the mid-thoracic region (only for thoracic and thoracolumbar scoliotic curvatures)

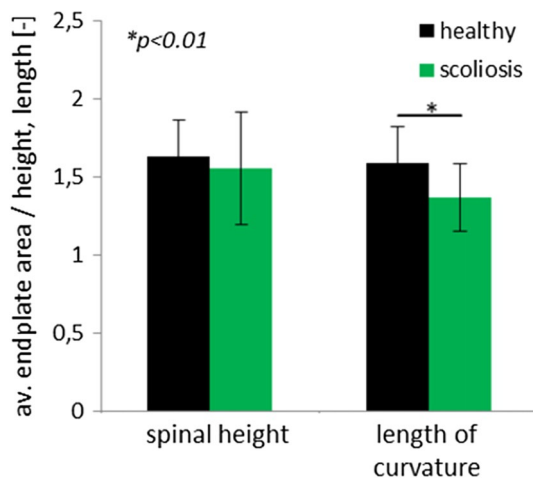


Fig. 5 Relation between average endplate area and the spinal height, respectively, the length of the curvature, for healthy and scoliotic spines

within the AIS group, once the endplate area was compared with the length of the curvature.

Spinal displacement

The lateral displacement of the scoliotic spine was significantly different in relation to the healthy spines depending on the position of the main scoliotic curvature (Fig. 6a). In the lumbar AIS group, lateral offset was significantly different within the lumbar levels and at T2, whereas the thoracic group exhibited significant differences in all levels between T4 and L5, except for T12.

Axial rotation

Our analyses revealed that axial rotation increased towards the apex vertebra of the scoliotic curvature (Fig. 6b), whereas the rotational peak depends on the type of scoliotic curvature. For lumbar AIS, the values ranged from $-8.9^{\circ} \pm 8.1^{\circ}$ at T7 and $32.7^{\circ} \pm 5.3^{\circ}$ at L1; for thoracic AIS, the values ranged between $-20.7^{\circ} \pm 14.1^{\circ}$ at T9 and

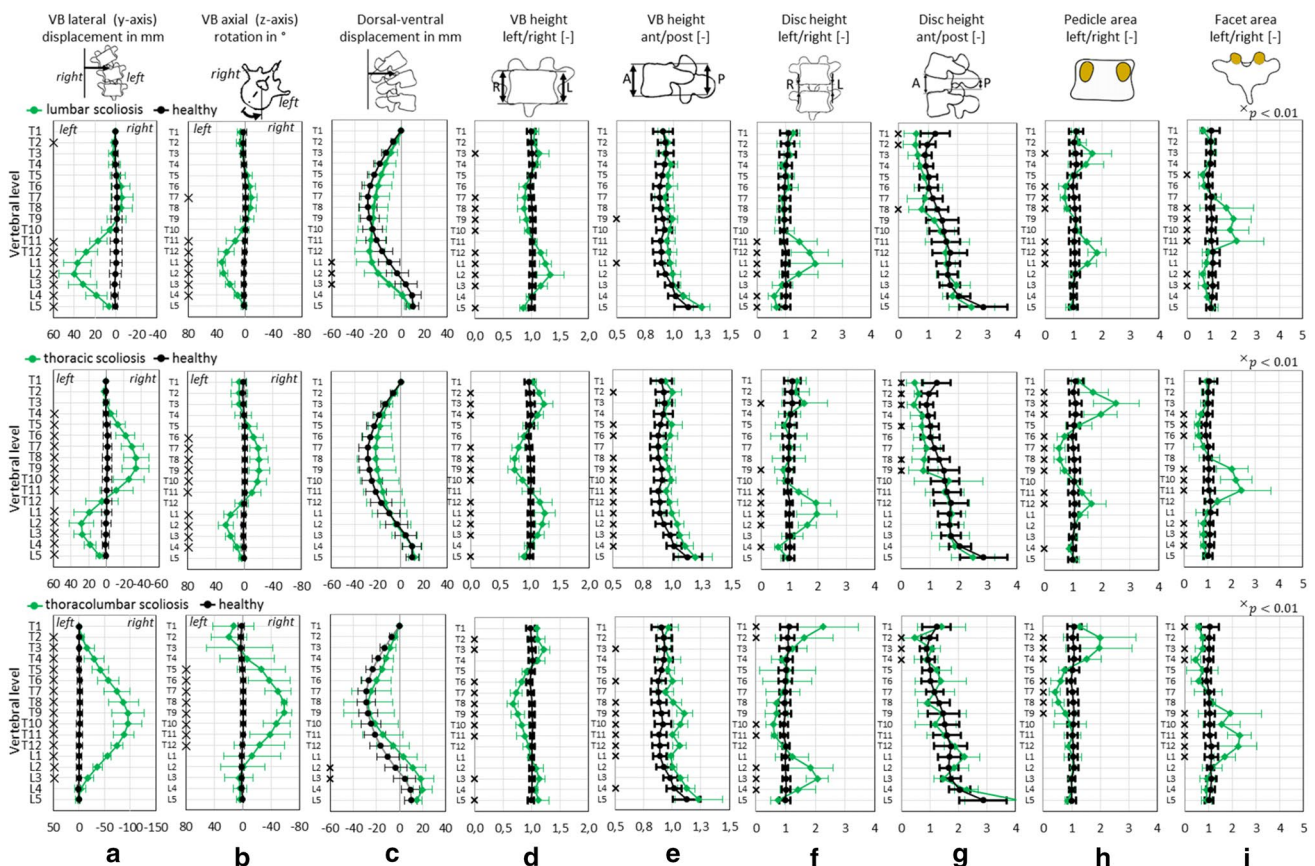


Fig. 6 Nine morphology parameters (a–i) and their development along the spinal levels for healthy spines (black) and scoliotic spines (green). Scoliotic spines were grouped depending on the position of

the main scoliotic curvature: top lumbar AIS, middle row thoracic AIS and bottom row thoracolumbar AIS

$25.9^\circ \pm 10.5^\circ$ at L2. At the thoracolumbar AIS, a main peak at T9 with $-58.5^\circ \pm 11.0^\circ$ was measured.

Dorsal–ventral displacement

Scoliotic spines generally revealed a reduced kyphosis within the thoracic region, whereas in the lumbar area, the spinal shape in the sagittal plane depended on the type of scoliosis (Fig. 6c): Lordosis was decreased significantly at the levels L1 to L3 in lumbar scoliosis types, while lordosis was increased in thoracolumbar scoliosis.

Shape of the vertebral body

Wedging of vertebral body was significantly pronounced in all three scoliotic types in the thoracic region between T7 and T10, with a lower vertebral body height on the left (concave) side compared to the right (convex) side of the curvature and a minimal ratio of 0.67 ± 0.1 at T8 in the thoracolumbar AIS group (Fig. 6d). This relation was reversed in the lumbar region for lumbar and thoracic AIS cases, with maximal values of 1.25 ± 0.16 .

The relation between the anterior and posterior vertebral body heights was generally higher in scoliotic spines than in healthy spines (Fig. 6e). Compared to the posterior height, the anterior height in scoliotic spines was lower in the upper thoracic region (min. 0.91 ± 0.05). In the lumbar region, the heights were equal or in an opposite relation to the thoracic region, with a maximum of about 1.25 ± 0.07 .

Shape of the intervertebral disc

Lateral wedging of the disc was significant in the lumbar region with a maximal value of 2.06 ± 0.37 in thoracolumbar AIS group (Fig. 6f). The relation between the anterior and posterior disc heights was overall reduced within the thoracic levels T1 to T9 in the AIS groups in comparison with healthy spines (Fig. 6g).

Articular facet joint area

The superior facet joint areas exhibited differences especially in the lower thoracic region between T8 and T12, with a relation of 2.3 ± 0.5 (Fig. 6h). This relation was reversed above and below this spinal region, which resulted in a smaller facet area on the left side compared to the right facet (min. 0.5 ± 0.2 at T4 for thoracolumbar AIS).

Pedicle cross-sectional area

Differences within the cross-sectional area of the pedicles between left and right sides are especially pronounced in the thoracic region, independent of the scoliotic type (Fig. 6i).

High peaks were measured around T3 (2.5 ± 0.79 for thoracic AIS), T7 (0.4 ± 0.19 at thoracolumbar AIS) and T12 (1.8 ± 0.3 at lumbar AIS).

Discussion

The presented results suggest that the development of morphological parameters along the spine depicts a characteristic pattern which reveals a distinct load path prevalent within scoliotic spines. The deformation of the spine relative to the sagittal plane of symmetry seems to go hand in hand with multiple changes within the bone morphology.

First it should be noted that even spines of the healthy group, classified as non-scoliotic, exhibited an inherent deformation and rotation of the spine, which qualitatively matched those found in scoliotic spines. These findings correspond to data measured by Kouwenhoven et al. [24], who also identified significant rotation of up to 2.7° of the vertebrae within the thoracic region of healthy patients.

The measurement of an increased length of the anterior column of scoliotic spines compared to healthy spines agrees with previous studies: the comparison of the anterior spinal length with the length of the spinal canal [19, 22], as well as the increased anterior compared to the posterior vertebral body height [25]. However, these results show no evidence that scoliosis is primarily *caused* by an asymmetric growth or tethering of the spinal canal. The morphological data suggest that an increase in height is more likely to be result of a natural adaption process. In contrast to the findings of Brink et al. [26], our data suggests that the anterior spinal overgrowth is primarily located in the vertebral body, rather than in the disc.

The observed increased spinal length and, concomitant, the reduced endplate area in scoliotic spines in comparison with the healthy control group might be explained by the Hueter–Volkman principle [27, 28] and Wolff's law [1]. The latter states that in a straight healthy spine the size of an endplate area would correlate with the axial load the vertebra is subjected to. A straight spine which is deformed from the symmetry plane would theoretically decrease in height, in case no bone adaptation process occurred. Nonetheless, the deformation alters load transmission, causing a reduction in the axial load component which acts vertically on the endplate surface. According to the Hueter–Volkman principle [29, 30], a decrease in the axial compression load would result in an increase in the height. This agrees with the finding of an increased vertebral body height in scoliotic spines. The overall length of spinal curvature increases in scoliotic spines and is, therefore, longer than healthy non-deformed spines.

The observed wedging of the vertebral body, as well as the size differences between the right and left facet areas

and pedicle sizes in AIS, suggests an uneven load sharing between and within the anterior and posterior columns. The pedicle size between the left and right sides deviates mainly at the apex of the scoliotic curvature, while the facet size varies especially in the region of the inflection point of the curvature (Fig. 7).

These findings suggest that the concave site of the vertebral body around the apex is subjected to higher loads. The site of loading on the articular facets changes above and below the apex. The observed deformation patterns of the spine might be a result of stresses originating from the rib cage [31].

Limitations

This study was mainly limited by the rather small patient number. Due to ethical concerns, CT images in high quality which cover the entire thoracic and lumbar spine including the chest are rarely taken. This makes the analysed images within this study an exceptional database.

Sources of error include the placement of the landmarks in particular on the scoliotic vertebrae, since the selection of the right, left and anterior vertebral edges on strongly distorted vertebrae proved to be challenging. These errors, however, should be captured by the quantified inter- and intra-rater variability.

Regarding the pathogenesis of scoliosis, the deformation of bony structures may very well be secondary, due to the distinct correlation between deformation and multiple

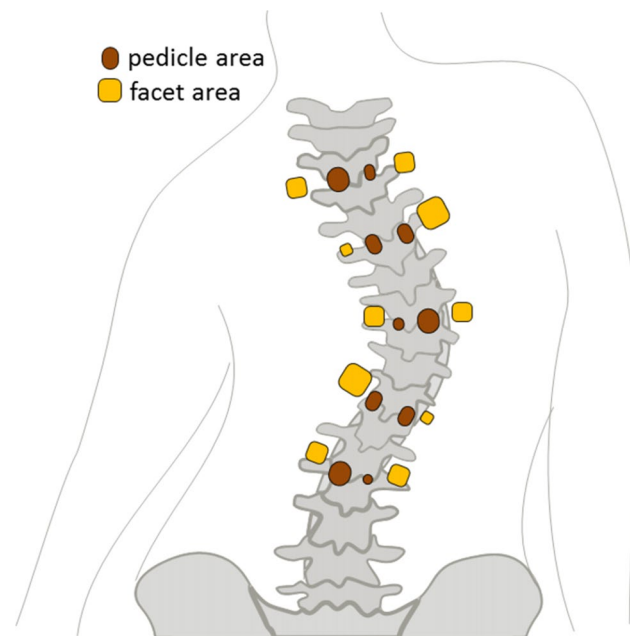


Fig. 7 Qualitative sketch of the variation of the pedicle and facet area size along a scoliotic curvature

morphological changes. A systemic asymmetrical load distribution may deform the spine and trigger the characteristic morphology pattern observed in scoliotic spines.

The presented morphology data can further provide an important basis for the development of scoliotic spine models.

Acknowledgements This work was supported by the German Research Foundation (DFG), Project WI 1352/20-1.

Compliance with ethical standards

Conflict of interest None of the authors has any potential conflict of interest.

References

1. Wolff J (1893) Das Gesetz der transformation der Knochen. *DMW—Dtsch Medizinische Wochenschrift* 19:1222–1224
2. Carter DR, Orr TE, Fyhrie DP (1989) Relationships between loading history and femoral cancellous bone architecture. *J Biomech* 22(3):231–244
3. Turner CH (1992) Functional determinants of bone structure: beyond Wolff's law of bone transformation. *Bone* 13(6):403–409
4. Wilke H-J, Mathes B, Midderhoff S, Graf N (2015) Development of a scoliotic spine model for biomechanical in vitro studies. *Clin Biomech* 30(2):182–187
5. Niemeyer F, Wilke H-J, Schmidt H (2012) Geometry strongly influences the response of numerical models of the lumbar spine—a probabilistic finite element analysis. *J Biomech* 45(8):1414–1423
6. Thong W, Parent S, Wu J, Aubin CE, Labelle H, Kadoury S (2016) Three-dimensional morphology study of surgical adolescent idiopathic scoliosis patient from encoded geometric models. *Eur Spine J* 25(10):3104–3113
7. Parent S, Labelle H, Skalli W, de Guise J (2004) Vertebral wedging characteristic changes in scoliotic spines. *Spine (Phila Pa 1976)* 29(20):E455–E462
8. Scherrer SA, Begon M, Leardini A, Coillard C, Rivard CH, Allard P (2013) Three-dimensional vertebral wedging in mild and moderate adolescent idiopathic scoliosis. *PLoS ONE* 8(8):1–7
9. Modi HN, Suh SW, Song HR, Yang JH, Kim HJ, Modi CH (2008) Differential wedging of vertebral body and intervertebral disc in thoracic and lumbar spine in adolescent idiopathic scoliosis—a cross sectional study in 150 patients. *Scoliosis* 3(1):11
10. Schlösser TPC, van Stralen M, Brink RC, Chu WCW, Lam T-P, Vincken KL, Castelein RM, Cheng JCY (2014) Three-dimensional characterization of torsion and asymmetry of the intervertebral discs versus vertebral bodies in adolescent idiopathic scoliosis. *Spine (Phila Pa 1976)* 39(19):E1159–E1166
11. Little JP, Percy MJ, Izatt MT, Boom K, Labrom RD, Askin GN, Adam CJ (2015) Understanding how axial loads on the spine influence segmental biomechanics for idiopathic scoliosis patients: a magnetic resonance imaging study. *Clin Biomech (Bristol, Avon)* 32(2016):220–228
12. Roaf R (1958) Rotation movements of the spine with special reference to scoliosis. *J Bone Joint Surg Br* 40-B(2):312–332
13. Kiefer A, Shirazi-Adl A, Parnianpour M (1998) Synergy of the human spine in neutral postures. *Eur Spine J* 7(6):471–479
14. Lowe T, Edgar M, Margulies J (2000) Etiology of idiopathic scoliosis: current trends in research. *J Bone Joint Surg* 82(8):1157

15. Davis CM, Grant CA, Pearcy MJ, Askin GN, Labrom RD, Izatt MT, Adam CJ, Little JP (2017) Is there asymmetry between the concave and convex pedicles in adolescent idiopathic scoliosis? A CT investigation. *Clin Orthop Relat Res* 475(3):884–893
16. Parent S, Labelle H, Skalli W, Latimer B, de Guise J (2002) Morphometric analysis of anatomic scoliotic specimens. *Spine (Phila Pa 1976)* 27(21):2305–2311
17. Tanabe H, Aota Y, Nakamura N, Saito T (2017) A histomorphometric study of the cancellous spinal process bone in adolescent idiopathic scoliosis. *Eur Spine J* 26(6):1600–1609
18. Wang ZW, Lee WYW, Lam TP, Yip BHK, Yu FWP, Yu WS, Zhu F, Ng BKW, Qiu Y, Cheng JCY (2017) Defining the bone morphometry, micro-architecture and volumetric density profile in osteopenic vs non-osteopenic adolescent idiopathic scoliosis. *Eur Spine J* 26(6):1586–1594
19. Porter R (2000) Idiopathic scoliosis: the relation between the vertebral canal and the vertebral bodies. *Spine (Phila Pa 1976)* 25(11):1360–1366
20. Chu WC, Yeung HY, Chau WW, Lam WW, Ng BK, Lam TP, Lee KM, Cheng JC (2006) Changes in vertebral neural arch morphology and functional tethering of spinal cord in adolescent idiopathic scoliosis—study with multi-planar reformat magnetic resonance imaging. *Stud Health Technol Inform* 123(1):27–33
21. Guo X, Chau WW, Chan YL, Cheng JCY (2003) Relative anterior spinal overgrowth in adolescent idiopathic scoliosis. Results of disproportionate endochondral-membranous bone growth. *J Bone Joint Surg Br* 85(7):1026–1031
22. Roth M (1981) Idiopathic scoliosis from the point of view of the neuroradiologist. *Neuroradiology* 21(3):133–138
23. Oliphant TE (2007) Python for scientific computing. *Comput Sci Eng* 9(3):10–20
24. Kouwenhoven J-WM, Bartels LW, Vincken KL, Viergever MA, Verbout AJ, Delhaas T, Castelein RM (2007) The relation between organ anatomy and pre-existent vertebral rotation in the normal spine: magnetic resonance imaging study in humans with situs inversus totalis. *Spine (Phila Pa 1976)* 32(10):1123–1128
25. Newell N, Grant CA, Keenan BE, Izatt MT, Pearcy MJ, Adam CJ (2016) Quantifying progressive anterior overgrowth in the thoracic vertebrae of adolescent idiopathic scoliosis patients: a sequential magnetic resonance imaging study. *Spine J* 41(7):E382–E387
26. Brink RC, Schlösser TPC, Colo D, Vavrouch L, Van Stralen M, Vincken KL, Malmqvist M, Kruyt MC, Tropp H, Castelein RM (2017) Anterior spinal overgrowth is the result of the scoliotic mechanism and is located in the disc. *Spine (Phila Pa 1976)* 42:818–822
27. Volkmann R (1869) Die Krankheiten der Bewegungsorgane. *Handb der Allg und Spez Chir Bd II, Abt 1:350–351*
28. Hueter C (1863) Anatomische Studien an den Extremitäten-gelenken Neugeborener und Erwachsener. *Arch f{ü}r Pathol Anat und Physiol und f{ü}r Klin Med* 26(5):484–519
29. Stokes IA, Spence H, Aronsson DD, Kilmer N (1996) Mechanical modulation of vertebral body growth. Implications for scoliosis progression. *Spine (Phila Pa 1976)* 21(10):1162–1167
30. Stokes IAF (2002) Mechanical effects on skeletal growth. *J Musculoskelet Neuronal Interact* 2(3):277–280
31. Schlager B, Niemeyer F, Galbusera F, Wilke HJ (2018) Asymmetrical intrapleural pressure distribution: a cause for scoliosis? A computational analysis. *Eur J Appl Physiol* (in press)

Affiliations

Benedikt Schlager¹ · Florian Krump¹ · Julius Boettinger¹ · Frank Niemeyer¹ · Michael Ruf² · Sebastian Kleiner³ · Meinrad Beer³ · Hans-Joachim Wilke¹

✉ Hans-Joachim Wilke
hans-joachim.wilke@uni-ulm.de

¹ Institute of Orthopaedic Research and Biomechanics, Centre for Trauma Research Ulm, Ulm University Medical Centre, Helmholtzstraße 14, 89081 Ulm, Germany

² SRH Klinikum Karlsbad-Langensteinbach gGmbH, Zentrum für Wirbelsäulenchirurgie, Orthopädie und Unfallchirurgie, Guttmannstraße 1, 76307 Karlsbad, Germany

³ Klinik für Diagnostische und Interventionelle Radiologie, Ulm University Medical Centre, Albert-Einstein-Allee 29, 89081 Ulm, Germany